18. ANTHROPOGENIC ENHANCEMENT OF MODERATE-TO-STRONG EL NIÑO EVENTS LIKELY CONTRIBUTED TO DROUGHT AND POOR HARVESTS IN SOUTHERN AFRICA DURING 2016

Chris Funk, Frank Davenport, Laura Harrison, Tamuka Magadzire, Gideon Galu, Guleid A. Artan, Shraddhanand Shukla, Diriba Korecha, Matayo Indeje, Catherine Pomposi, Denis Macharia, Gregory Husak, and Faka Dieudonne Nsadisa

A 40-member CESM LE ensemble indicates that climate change likely increased the intensity of the 2015/16 El Niño, contributing to further decreases in SA precipitation, crop production and food availability.

Introduction. In December–February (DJF) of 2015/16, a strong El Niño (Niño-3.4 SST >29°C) contributed to a severe drought over southern Africa (SA; Funk et al. 2016). A 9-million ton cereal deficit resulted in 26 million people in need of humanitarian assistance (SADC 2016). While SA rainfall has a well-documented negative teleconnection with Niño-3.4 SSTs (Hoell et al. 2015, 2017; Jury et al. 1994; Lindesay 1988; Misra 2003; Nicholson and Entekhabi 1987; Nicholson and Kim 1997; Reason et al. 2000; Rocha and Simmonds 1997), the link between climate change and El Niño remains unclear (Christensen et al. 2013) due to the large natural variability of ENSO SSTs (Wittenberg 2009), uncertainties surrounding measurements and trends (Solomon and Newman 2012), intermodel differences in ENSO representation and feedbacks (Guilyardi et al. 2012; Kim et al. 2014), and difficulties associated with quantifying ENSO strength (Cai et al. 2015).

AFFILIATIONS: Funk—U.S. Geological Survey, Center for Earth Resources Observation and Science, and UC Santa Barbara Climate Hazards Group, Santa Barbara, California; Davenport, Harrison, Shukla, Pomposi, and Husak—UC Santa Barbara Climate Hazards Group, Santa Barbara, California; Magadzire, Galu, and Korecha—UC Santa Barbara Climate Hazards Group, Santa Barbara, California, and Famine Early Warning Systems Network; Artan—Intergovernmental Authority on Development (IGAD) Climate Prediction & Applications Centre, Nairobi, Kenya; Indeje—IGAD USAID/Kenya and East Africa Planning for Resilience in East Africa Through Policy Adaptation, Research, and Economic Development, Nairobi, Kenya; Macharia—Regional Center for Mapping of Resources for Development, Nairobi, Kenya; Nsadisa—Director of the Southern African Development Community's Climate Services Centre.

DOI:10.1175/BAMS-D-17-0112.1

A supplement to this article is available online (10.1175/BAMS-D-17-0112.2)

Figure 18.1a highlights observational uncertainties (Compo and Sardeshmukh 2010; Solomon and Newman 2012) using four datasets: ERSSTv4 (Huang et al. 2015), HadISST (Rayner et al. 2003), Kaplan SST (Kaplan et al. 1998), and Hurrell (Hurrell et al. 2008). These products differ substantially in their representation of cool events and Niño-3.4 variance. Two SST products indicate significant upward trends; two SST products do not. These data have been standardized to remove systematic differences in variance.

Focusing just on the behavior of moderate–strong El Niño events (MSENEs), we can produce more robust (first order) statistics by comparing the means of the top ten warmest Niño-3.4 events between 1921–80 and the top six warmest events between 1981–2016. Rather than using a set SST threshold, MSENEs are defined as 1-in-6-year warm events. This provides a simple nonparametric approach that takes advantage of the well understood quasi-periodic nature of ENSO to identify MSENEs across multiple models and simulations. Modest changes in the number of events (say, 1-in-7 or 1-in-5) produced modest increases and decreases in El Niño temperatures, but did not substantially change the results.

We begin our analysis in 1921 (because ship data before 1921 is limited), and divide the remaining 96 years into two time periods with relatively weak and strong radiative forcing, respectively. Examining changes in MSENE means (horizontal lines in Fig. 18.1a), we find that all the observational datasets identify significant increases (Fig. ES18.1 examines ERSSTv4 errors). Note that we are not explicitly examining changes in ENSO variance, ENSO means, or Niño-3.4 SST trends, but only Niño-3.4 magnitudes

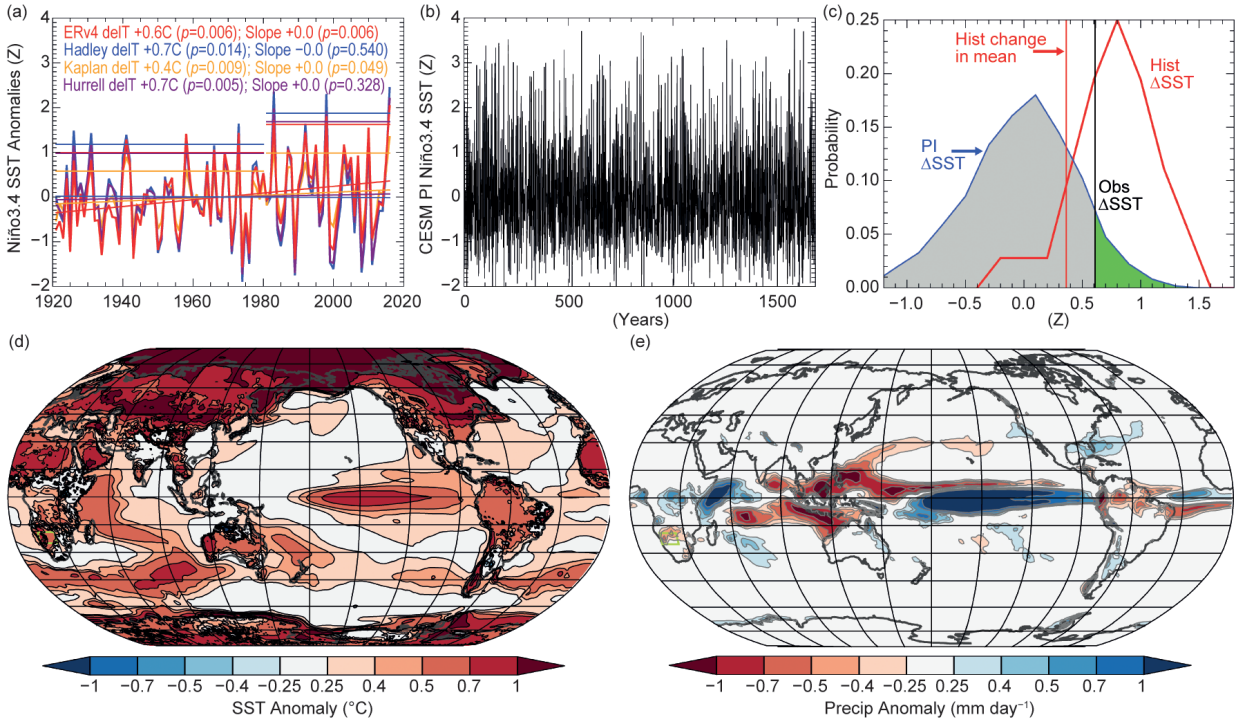

Fig. 18.1. (a) Observed NINO3.4 SST (Z) from four sources, trend lines, and changes in 1-in-6-year maximum Niño-3.4 seasons. (b) 1700 years of DJF Niño-3.4 SSTs (Z) from the CESM1 PI simulation. (c) PI and Historic distributions of changes in 1-in-6-year maximum NINO3.4 SST. Gray/green shading denotes likelihood given PI conditions. (d),(e) Composites of CESM Historic simulation SST (°C) and precipitation (mm day^{-1}), respectively, for the top 1-in-6 1981–2016 NINO3.4 SST seasons and the top 1921–80 seasons. These are based on the mean of 6 × 40 events and 10 × 40 events.

during MSENEs. We will use a 40-member ensemble of simulations from the CESM1 Large Ensemble (LE) project (Kay et al. 2015) to contrast SA rainfall during MSENEs based on historic simulations forced with greenhouse gasses and aerosols with simulated precipitation under preindustrial (PI) conditions.

ENSO exhibits large natural variations in amplitude (Wittenberg 2009). Figure 18.1b shows Niño-3.4 SST from 1700 years of CESM LE PI simulations. Even without climate change, we find Niño-3.4 SST anomalies greater than +3°Z (where Z denotes a standardized anomaly), sometimes occurring in sequence. To derive a PI sampling distribution that mimics Fig. 18.1a, we calculate 10 000 sample changes in 1-in-6-year maximum SST, based on sequential periods of 60 and 36 years, drawn from the 1700 year CESM1 PI simulation. Large changes can occur through nonanthropogenic processes (Fig. 18.1c). We use this PI distribution to assess the likelihood of the observed ~+0.61° ± 0.18°C temperature difference for MSENEs in the two composites. Such a change would be possible but *very unlikely* under PI conditions (only 7% of the PI simulations warmed this much). While unlikely, such an event is certainly plausible in a world without climate change.

Using 40 simulations from the CESM LE experiment, we can also derive a PDF of 1981–2016 versus 1921–80 El Niño SSTs (Fig. 18.1c). An animation of these individual simulations can be found at https://tinyurl.com/Niño3-4-sims-gif. Contrasting the variance of the 1981–2016 historic versus PI Niño-3.4 CESM LE SST time series, we find a substantial (55%) increased in variance (from 1.23°C^2 to 1.91°C^2, $p = 0.0001$). Not all simulations produced an increase, and the PI and historical PDFs overlap substantially. Overall, however, we find a substantial (+0.75°C average change) and significant ($p = 0.0001$, d.f. 638) increase in MSENE Niño-3.4 SST, which appears to be only partially explained by a shift in the overall mean between 1921–80 and 1981–2016 (+0.36°C). The 95% confidence intervals of this estimated change are large 0.0 to +1.3°C. Under PI conditions, the observed +0.61°C warming would be *very unlikely* ($p = 6\%$). Based on the historical climate change PDF, warming of +0.61°C or more would be *likely*. A 53-member multimodel ensemble also shows substantial and

significant Niño-3.4 SST increases). This 53-member multimodel ensemble indicates that 1981–2016 MSENEs would be +0.58°C warmer.

These results appear consistent with recent model analyses showing an increase in the frequency of strong El Niño events with greenhouse warming (Cai et al. 2015) and 1920–2040 ENSO amplitude (Kim et al. 2014), and reconstructions of paleo-ENSO variance at centennial (Li et al. 2013; McGregor et al. 2013) and millennial (Cobb et al. 2003) time scales. Figures 18.1d, e show changes in the CESM1 historic El Niño SST and precipitation; the CESM simulations indicate substantial increases in zonal and meridional SST gradients and equatorial rainfall anomalies, both of which are features of stronger ENSO forcing (Cai et al. 2015). CAM5 simulations based on observed SSTs show similar precipitation changes (Fig. ES18.2).

SA and Niño-3.4 rainfall analysis. This section examines SA and NINO3.4 precipitation from CESM LE PI and historical precipitation simulations[1]. Figure 18.2a shows the SA and NINO3.4 precipitation PDFs associated with MSENEs. Precipitation increases in Niño-3.4 excites equivalent barotropic Rossby wave trains (Hoskins and Karoly 1981) that increase the frequency of SA drought (Hoell et al. 2015). The risk ratio for strong Niño-3.4 precipitation events (>1Z-score, or standardized anomaly) was 181%. The risk ratio is the ratio of the event probability in the real world and 'natural' world without climate change influences (Easterling et al. 2016).

The PDFs of SA rainfall indicate substantial uncertainty, underscoring the complexity of SA rainfall, internal atmospheric variability, and the partial influence of ENSO, which describes about ~50% of the SA rainfall variance (Funk et al. 2016). Both the PI and historic ensembles have substantial spread, but the historic PDF is shifted to the left, indicating an increased chance of droughts during El Niño events. The risk ratio for droughts less than −1Z is 160%. A two-sample *t*-test indicates a very significant change (−0.6Z, $p = 0.0001$), with 95% confidence intervals of −0.4Z to −0.8Z. Given the inherent complexities in ENSO and a limited observational record to place the 2015/16 event in a broader historical context, we cannot be sure that SSTs in the Niño-3.4 region during recent MSENEs were not higher due to internal variability (noise). Still, utilizing tools like the CESM LE project, we can conclude that there is a likely shift towards higher Niño-3.4 SSTs and precipitation, and lower SA rainfall outcomes in the later MSENEs compared to earlier ones and that this is related to anthropogenic forcing. Examining the probabilities of the observed −1.7Z rainfall deficit based on the PI and historic distributions, we find that a drought of this severity would be possible but very unlikely under PI conditions (probability ~9%) and unlikely under historic conditions (probability ~20%).

Food security analysis—southern Africa. We relate changes in SA rainfall to changes in crop production. The major sources of uncertainty in this assessment

[1]We use a box for SA that is slightly to the west (19°–25°S, 15°–25°E) of the region used Funk et al. 2016, because rainfall simulations from the atmospheric component of the CESM1 (CAM5) displace the SA ENSO teleconnection slightly to the west (Fig. ES18.2).

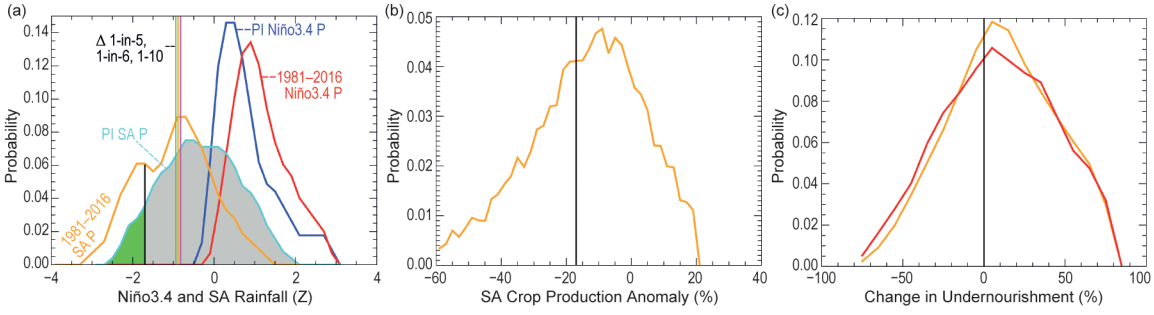

Fig. 18.2. (a) Precipitation attribution results. Standardized CESM SA and Niño-3.4 MSENE precipitation (Z) PDFs for PI and 1981–2016 Historic ensembles. Historic MSENE ensemble was based on 15% of 40 simulations for 36 years (216 El Niño events). Also shown are results based on 10% and 20%. PI ensemble used 15% of 1680 years (252 El Niño events). Green and gray shading indicates the probability of the observed −1.7Z drought occurring within the PI distribution. (b) Bootstrapped distribution of SA crop production anomalies (%), based on the PI and Historic SA precipitation distributions from (a), and the slope coefficient sampling distribution. Anomalies based on 2008–13 averages. (c) PDFs of changes in undernourishment (%) in Zimbabwe and Malawi, based on (b) and an FAO percent undernourished estimation procedure.

are 1) the uncertainty associated with SA rainfall changes, and 2) uncertainty in the relationship between SA rainfall and crop production. A regression between detrended 1981–2016 southern African[2] crop production and SA rainfall exhibited a significant but modest relationship (slope = +13.5% per 1Z, $R^2 = 0.42$), with a considerable standard error (3.7% per Z). To capture these uncertainties, we use a Monte Carlo sampling strategy based on 10 000 samples. For each sample we drew one CESM SA rainfall value out of the 240 1981–2016 El Niño samples ($R_{1981–2016}$), one rainfall outcome from the 280 PI SA El Niño rainfall values (R_{PI}), and one regression slope value (S) from a normal distribution with a mean of 13.5 and a standard deviation of 3.7. A production change value was then estimated as $(R_{1981–2016} - R_{PI})S$. This was repeated 10 000 times. As shown in Fig. 18.2b these estimates exhibit a high degree of uncertainty. The 95% confidence intervals range from −48% to 21%, with a median impact of −11%. The observed 2016 production anomaly was −17%. Seventy-four percent of these estimates were below normal, suggesting that it was *likely* that anthropogenic SA rainfall reductions also reduced SA crop production. Repeating this analysis for 1-in-10 and 1-in-5-year El Niño events produced similar results. It should be noted that the CAM5/CESM models tend to displace the SA rainfall anomalies to the west, indicating that the models do not perfectly capture the regional climatology. Observational studies, however, have produced results consistent with those presented here (Funk et al. 2016; Hoell et al. 2015; Ratnam et al. 2014).

Focusing on Zimbabwe and Malawi, large countries that rely on local production, we estimate changes in the undernourished population by translating production losses (Fig. 18.2b) into changes in the percent of the population estimated to be undernourished (FAO 2008). The broad uncertainty in production impacts translates into a wide spread of possible changes in undernourishment (Fig. 18.2c). These results indicate a median increase of the percent undernourished population to be 15% in Zimbabwe and 18% in Malawi, but the uncertainty surrounding these estimates is very high.

Conclusion. While the high natural variability of Niño-3.4 SSTs and the complexities surrounding both ENSO and climate change and ENSO/SA teleconnections make analyzing ENSO/SA/climate change difficult, the large CESM LE ensemble provides an exciting new resource. These simulations suggest that the recent increases in MSENE Niño-3.4 SST would be possible but *unlikely* under PI conditions and *likely* in historic climate change conditions. The CESM1 simulations suggest that some of this warming (+0.36°C) is associated with a trend towards warmer Niño-3.4 conditions, but we find additional warming that may be associated with an amplification of strong ENSO responses (Cai et al. 2015) and east Pacific precipitation (Cai et al. 2015). Contrasts between PI and historic SA and Niño-3.4 El Niño precipitation events show *likely* decreases and increases, respectively. Contributions to increased crop deficits are also found to be likely, but with a large spread of possible outcomes. While the large number of available CESM and CAM5 simulations allowed us to examine in depth responses in a single atmospheric model, more research with more models will be needed to validate the results. It should also be noted that this study has not focused on the future average climate; we are not suggesting that the future average climate will look more El Niño-like. It should also be noted that while observational analyses support stronger SA drought signals during strong canonical El Niño events (Hoell et al. 2015; Ratnam et al. 2014), Indian Ocean SST patterns also influence regional precipitation (Goddard and Graham 1999; Hoell et al. 2017); these influences have not been factored into this analysis.

ACKNOWLEDGMENTS. This research was supported by the U.S. Geological Survey's Land Change Science program, the USAID Famine Early Warning Systems Network, and NASA SERVIR grant NNX16AM02G. Production of the rainfall data was supported by the USGS Earth Resources Observations and Science Center (http://earlywarning.usgs.gov / fews/datadownloads/Global/CHIRPS2.0). We would like to thank the Royal Netherlands Meteorological Institute for providing the CMIP5 simulations (https://climexp.knmi.nl) and the Earth System Research Laboratory Physical Sciences Division (www.esrl.noaa.gov/) for providing access to the CESM1 LENS simulations, and the Large Ensemble Community Project for producing the simulations (www.cesm.ucar.edu/projects /community-projects/LENS/).

[2] South Africa, Lesotho, Swaziland, Botswana, Zambia, Mozambique, Malawi, and Zimbabwe.

REFERENCES

Cai, W., and Coauthors, 2015: ENSO and greenhouse warming. *Nat. Climate Change*., **5**, 849–859, doi:10.1038/nclamite2743.

Christensen, J. H., and Coauthors, 2013: Climate phenomena and their relevance for future regional climate change. *Climate Change 2013: The Physical Science Basis*, T. Stocker et al., Eds., Cambridge University Press, 1217–1308.

Cobb, K. M., C. D. Charles, H. Cheng, and R. L. Edwards, 2003: El Niño/Southern Oscillation and tropical Pacific climate during the last millennium. *Nature*, **424**, 271–276, doi:10.1038/nature01779.

Compo, G. P., and P. D. Sardeshmukh, 2010: Removing ENSO-related variations from the climate record. *J. Climate*, **8**, 1957–1978, doi:10.1175/2009JCLI2735.1.

Easterling, D. R., K. E. Kunkel, M. F. Wehner, and L. Sun, 2016: Detection and attribution of climate extremes in the observed record. *Wea. Climate Extremes*, **11**, 17–27, doi:10.1016/j.wace.2016.01.001.

FAO, 2008: FAO Methodology for the Measurement of Food Deprivation: Updating the minimum dietary energy requirements. United Nations Food and Agriculture Organization. [Available online at www.fao.org/fileadmin/templates/ess/documents/food_security_statistics/metadata/undernourishment_methodology.pdf.]

Funk, C., L. Harrison, S. Shukla, A. Hoell, D. Korecha, T. Magadzire, G. Husak, and G. Galu, 2016: Assessing the contributions of local and east Pacific warming to the 2015 droughts in Ethiopia and southern Africa [in "Explaining Extreme Events of 2015 from a Climate Perspective"]. *Bull. Amer. Meteor. Soc.*, **97** (12), S75–S80, doi:10.1175/BAMS-D-16-0167.1.

Goddard, L., and N. E. Graham, 1999: Importance of the Indian Ocean for simulating rainfall anomalies over eastern and southern Africa. *J. Geophys. Res.*, **104**, 19,099–19,116, doi:10.1029/1999JD900326.

Guilyardi, E., H. Bellenger, M. Collins, S. Ferrett, W. Cai, and A. Wittenberg, 2012: A first look at ENSO in CMIP5. *CLIVAR Exchanges No.58*, **17** (1), 29–32.

Hoell, A., C. Funk, T. Magadzire, J. Zinke, and G. Husak, 2015: El Niño–Southern Oscillation diversity and southern Africa teleconnections during austral summer. *Climate Dyn.*, **45**, 1583–1599, doi:10.1007/s00382-014-2414-z.

——, ——, J. Zinke, and L. Harrison, 2017: Modulation of the Southern Africa precipitation response to the El Niño Southern Oscillation by the subtropical Indian Ocean dipole. *Climate Dyn.*, **48**, 2529–2540, doi:10.1007/s00382-016-3220-6.

Hoskins, B. J., and D. J. Karoly, 1981: The steady linear response of a spherical atmosphere to thermal and orographic forcing. *J. Atmos. Sci.*, **38**, 1179–1196, doi:10.1175/1520-0469(1981)038<1179:TSLROA>2.0.CO;2.

Huang, B., and Coauthors, 2015: Extended reconstructed sea surface temperature version 4 (ERSST. v4). Part I: upgrades and intercomparisons. *J. Climate*, **28**, 911–930, doi:10.1175/JCLI-D-14-00006.1.

Hurrell, J. W., J. J. Hack, D. Shea, J. M. Caron, and J. Rosinski, 2008: A new sea surface temperature and sea ice boundary dataset for the Community Atmosphere Model. *J. Climate*, **21**, 5145–5153, doi:10.1175/2008JCLI2292.1.

Jury, M., C. Mc Queen, and K. Levey, 1994: SOI and QBO signals in the African region. *Theor. Appl. Climatol.*, **50**, 103–115,doi:10.1007/BF00864907.

Kaplan, A., M. A. Cane, Y. Kushnir, A. C. Clement, M. B. Blumenthal, and B. Rajagopalan, 1998: Analyses of global sea surface temperature 1856–1991. *J. Geophys. Res.*, **103**, 18,567–18,589, doi:10.1029/97JC01736.

Kay, J., and Coauthors, 2015: The Community Earth System Model (CESM) large ensemble project: A community resource for studying climate change in the presence of internal climate variability. *Bull. Amer. Meteor. Soc.*, **96**, 1333–1349, do:10.1175/BAMS-D-13-00255.1.

Kim, S. T., W. Cai, F.-F. Jin, A. Santoso, L. Wu, E. Guilyardi, and S.-I. An, 2014: Response of El Niño sea surface temperature variability to greenhouse warming. *Nat. Climate Change*, **4**, 786–790, doi:10.1038/nclimate2326.

Li, J., and Coauthors, 2013: El Niño modulations over the past seven centuries. *Nat. Climate Change*, **3**, 822–826, doi:10.1038/nclimate1936.

Lindesay, J., 1988: South African rainfall, the Southern Oscillation and a Southern Hemisphere semi-annual cycle. *J. Climatol.*, **8**, 17–30, doi:10.1002/joc.3370080103.

McGregor, S., A. Timmermann, M. England, O. E. Timm, and A. Wittenberg, 2013: Inferred changes in El Niño–Southern Oscillation variance over the past six centuries. *Climate Past*, **9**, 2269–2284, doi:10.5194/cp-9-2269-2013.

Misra, V., 2003: The influence of Pacific SST variability on the precipitation over southern Africa. *J. Climate*, **16**, 2408–2418, doi:10.1175/2785.1.

Nicholson, S. E., and D. Entekhabi, 1987: Rainfall variability in equatorial and southern Africa: Relationships with sea surface temperatures along the southwestern coast of Africa. *J. Appl. Meteor.*, **26**, 561–578, doi:10.1175/1520-0450(1987)026<0561:RVIEAS>2.0.CO;2.

——, and J. Kim, 1997: The relationship of the El Niño-Southern Oscillation to African rainfall. *Int. J. Climatol.*, **17**, 117–135.

Ratnam, J. V., S. K. Behera, Y. Masumoto, and T. Yamagata, 2014: Remote effects of El Niño and Modoki events on the austral summer precipitation of southern Africa. *J. Climate*, **27**, 3802–3815, doi:10.1175/JCLI-D-13-00431.1.

Rayner, N., D. E. Parker, E. B. Horton, C. K. Follard, L. V. Alexander, D. P. Rowell, E. C. Kent, and A. Kaplan, 2003: Global analyses of sea surface temperature, sea ice, and night marine air temperature since the late nineteenth century. *J. Geophys. Res.*, **108**, 4407, doi:029/2002JD002670.

Reason, C., R. Allan, J. Lindesay, and T. Ansell, 2000: ENSO and climatic signals across the Indian Ocean basin in the global context: Part I, Interannual composite patterns. *Int. J. Climatol*, **20**, 1285–1327.

Rocha, A., and I. Simmonds, 1997: Interannual variability of south-eastern African summer rainfall. Part I: Relationships with air-sea interaction processes. *Int. J. Climatol.*, **17**, 235–265.

SADC, 2016: SADC Regional Vulnerability Assessment and Analysis Synthesis Report 2016: State of Food Insecurity and Vulnerability in the Southern African Development Community. Southern African Development Community, 65 pp. [Available online at www.sadc.int/documents-publications/show/4720.]

Solomon, A., and M. Newman, 2012: Reconciling disparate twentieth-century Indo-Pacific ocean temperature trends in the instrumental record. *Nat. Climate Change*, **2**, 691–699, doi:10.1038/nclimate1591.

Wittenberg, A. T., 2009: Are historical records sufficient to constrain ENSO simulations? *Geophys. Res. Lett.*, **36**, L12702, doi:10.1029/2009GL038710.